# ACCURACY OF OUTDOOR SOUND PROPAGATION PREDICTION IN A COMPLEX ENVIRONMENT USING SOME REFERENCE NUMERICAL MODELS

François ABALLEA[1], Jérôme DEFRANCE[1],
Marine BAULAC[1], Mathieu FOURNIER[2]

[1] *Centre Scientifique et Technique du Batiment (CSTB), Acoustics and Ligthing Department, 24 rue Joseph Fourier, 38400 Saint Martin d'Hères, FRANCE*

[2] *Centres d'Etudes Techniques de l'Equipement (CETE) de Lyon, Boulevard de l'industrie, BP 141, 71404 Autun Cedex, FRANCE*

## SUMMARY

The paper presents principles which can be used in reference numerical models to make easy calculations for predicting long-range outdoor sound propagation under complex environment. Limits, assumptions as well as approximations used are discussed here in terms of accuracy for typical road traffic configurations, depending on range of frequency, geometry of the site and atmospheric conditions. Part of this work has been achieved during the European Project Harmonoise.

## INTRODUCTION

Several principles are introduced and discussed here. The application of an average ground effect instead of a mixed ground for ground impedance description, the importance of the reflection order in GFPE-Kirchhoff approach, the error due to the used of a range independent wind speed profile instead of an evolutive one, the interest of 2D models instead of 3D models, a method allowing shifting from a logarithmic sound speed profile to a linear sound speed profile are presented. The aim of those principles is to reduce calculation time consuming for outdoor sound propagation prediction in a complex environment with reference numerical models and to overcome some reference models limitations. Each time principles are applied to road traffic configurations.

## GROUND EFFECT

### Introduction

The case of mixed ground is often encountered in outdoor sound propagation. Most of time two types of surfaces have to be considered: an absorbing one made of soil with vegetation on it (grass, plants) and a reflective one made of asphalt, concrete or stone. The change of surface type does not necessarily correspond to the change of topography. Moreover, along a path, there may be many successive different types at the same level. The calculations are achieved in a homogeneous atmosphere using MICADO, a 2D BEM computational code [1]. The two types of ground are modelled here by two impedances: an infinite one for the rigid case, and one calculated with the Delany and Bazley's model [2] with an air flow resistivity of 200 kPa.s.m$^{-2}$. The first simulations concern a ground made of 50% of reflective and 50% of absorbing parts. A few more calculations are also presented for 33% and 67% of absorbing parts.

## Configurations and results

The monopole source is 0.5 m high. The receiver is 2 m high and 100 m away from the source (horizontal distance). The "100 m" of propagation are divided in regular reflective and absorbing successive strips. Ground "before" source and "after" receiver is rigid.

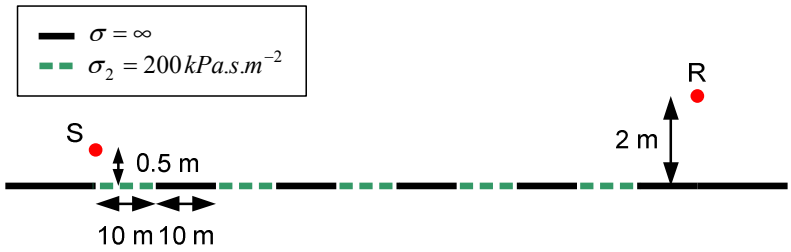


*Figure 1: Example of configuration (case 8)*

The calculations are achieved from 50 to 5000 Hz for each mid 3rd octave band frequency. Different cases are studied. For quite small strips:

- Case 1: 0.5 m wide strips (first strip "after" source is reflective),
- Case 2: 0.5 m wide strips (first strip "after" source is absorbing),
- Case 3: 1 m wide strips (first strip "after" source is reflective),
- Case 4: 1 m wide strips (first strip "after" source is absorbing),

For wider strips:

- Case 5: 5 m wide strips (first strip "after" source is reflective),
- Case 6: 5 m wide strips (first strip "after" source is absorbing),
- Case 7: 10 m wide strips (first strip "after" source is reflective),
- Case 8: 10 m wide strips (first strip "after" source is absorbing),

Another couple of configurations have been investigated with strips of width 1 m and 2 m alternatively.

- Case 9: 1 and 2 m successive wide strips (first 1 m strip is absorbing, ie. 33% of absorbing parts),
- Case 10: 1 and 2 m successive wide strips (first 1 m strip is reflective, ie. 67% of absorbing parts)

The results are given in terms of excess attenuation as a function of frequency in the following Figures. The tables below show for each set of cases the closest equivalent resistivity calculated by dichotomy (rounded by 10 kPa.s.m$^{-2}$) for each octave band mid frequency.

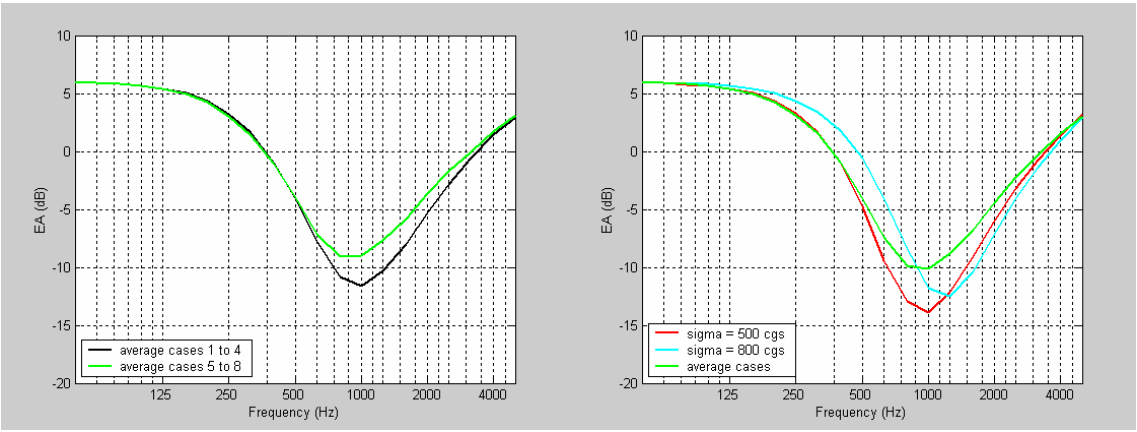


*Figure 2: Average Excess Attenuation as a function of frequency for cases 1 to 4 and 5 to 8 (left) and for cases 1 to 8 compared to two different homogeneous ground configurations results*

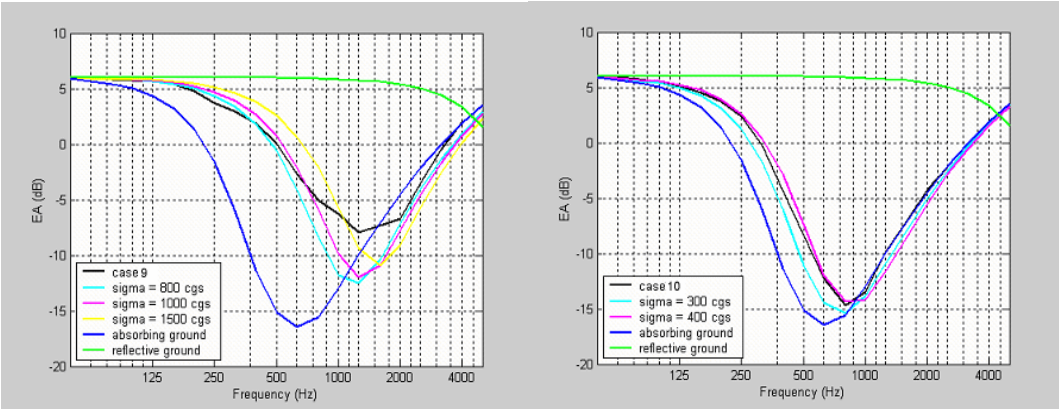


*Figure 3: Excess Attenuation as a function of frequency for case 9 (33% abs) (left) and case 10 (67% abs) (right) compared to different homogeneous ground configurations results*

*Table 1: Closest equivalent resistivity calculated by dichotomy (rounded by 10 kPa.s.m$^{-2}$) for each octave band mid frequency*

| | $\sigma_{eq}$ (kPa.s.m$^{-2}$) | | | | |
|---|---|---|---|---|---|
| Freq. (Hz) | Cases 1 to 4 | Cases 5 to 8 | Cases 1 to 8 | Case 9 | Case 10 |
| 125 | 500 | 470 | 480 | > 5000 | 340 |
| 250 | 480 | 460 | 470 | 590 | 380 |
| 500 | 530 | 540 | 540 | 890 | 370 |
| 1000 | 820 | 1090 | 970 | 1420 | 250 |
| 2000 | 360 | 70 | 180 | 670 | 140 |

## Discussion and conclusions

Table 2 gives the trends of equivalent values of resistivity as a function of percentage of absorbing parts. Those average values have been obtained from the configurations described above with several heights of receiver and source. For normalized sound spectrum [3], calculations error between real cases and the average ground method is each time less than **0.3 dB(A)**. Thus, this approach allows to reduce calculation time in some reference models (example: BEM calculations) and overcome some reference models limitations (example: FFP calculations).

*Table 2: Equivalent values of resistivity as a function of percentage of absorbing parts*

| Percentage of absorbing parts | 125, 250 and 500 Hz | 1000 and 2000 Hz |
|---|---|---|
| 100% | $\sigma_{eq}$ = 200 kPa.s.m$^{-2}$ | $\sigma_{eq}$ = 200 kPa.s.m$^{-2}$ |
| 67% | $\sigma_{eq}$ = 400 kPa.s.m$^{-2}$ | $\sigma_{eq}$ = 300 kPa.s.m$^{-2}$ |
| 50% | $\sigma_{eq}$ = 500 kPa.s.m$^{-2}$ | $\sigma_{eq}$ = 800 kPa.s.m$^{-2}$ |
| 33% | $\sigma_{eq}$ = 800 kPa.s.m$^{-2}$ | $\sigma_{eq}$ = 1500 kPa.s.m$^{-2}$ |
| 0% | $\sigma_{eq} = \infty$ | $\sigma_{eq} = \infty$ |

# MULTI-REFLECTION ORDER

## Introduction

In this approach, backscattering created by reflections on vertical obstacle is considered by using a complementary Kirchhoff approximation called GFPE-Kirchhoff [4]. This method allows solving multi-reflection problems by choosing the order of reflection. We study here the effect of this reflection order. Calculations are achieved in homogeneous atmosphere using ATMOS [4] [5], a PE computational code conjointly developed by CSTB and CEA, and compared with MICADO [1].

## Configuration and results

A source located between two vertical barriers is studied. The calculation principle is to build image-sources $S'$ relatively to barrier vertical plane. For any reflections, the sound pressure at any calculation points above the obstacle is set to zero and then propagated to the receiver. The geometry and the calculation principle for an order of reflection of 2 is described Figure 4. In this case, the total pressure at the receiver is the sum of 3 fields: (a) diffracted, (b) simply reflected and diffracted and (c) double reflected and diffracted. Results for order of 1, 6 and 20 are compared to MICADO calculation Figure 5.

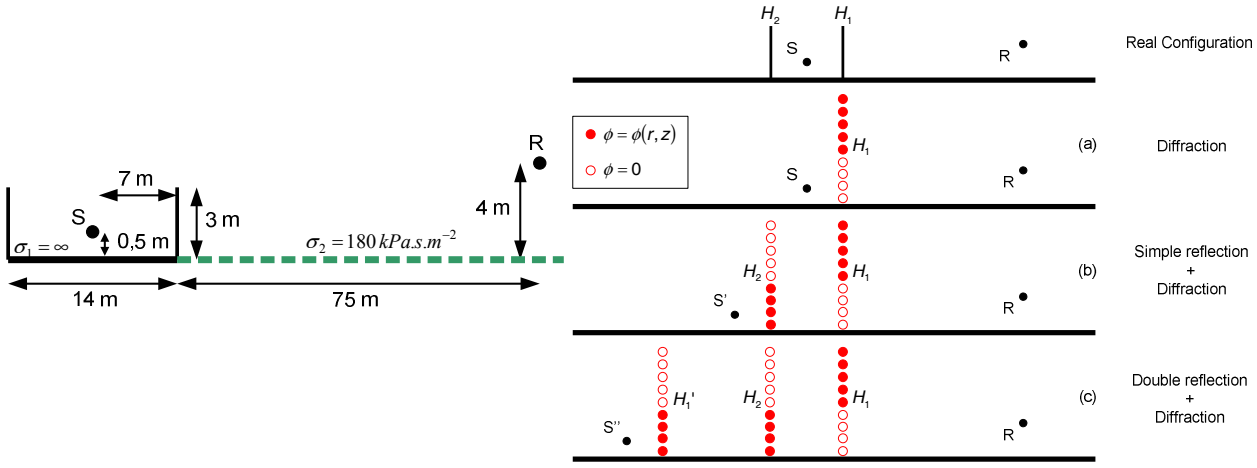


*Figure 4: Road traffic geometry (left) and principle of calculation at the order of 2 (right)*

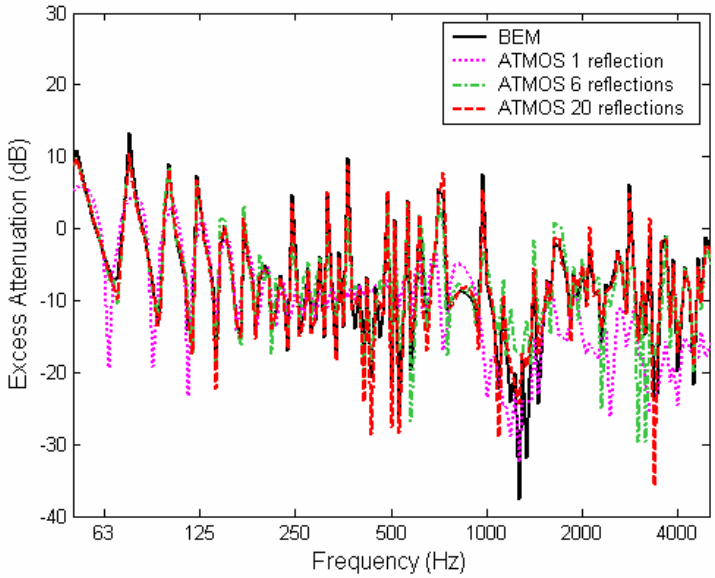


*Figure 5: Excess attenuation as a function of frequency for different reflection order*

## Discussion and conclusions

Results show the importance of the number of reflections to take into account. This number grows up with frequency: only 6 reflections are useful for frequencies lower than 1000 Hz instead of 20 for higher frequencies. However, for an emission spectrum [3] of a normalized traffic noise, the global excess attenuation error between a 6 and 20 reflections order is less than **0.5 dB(A)** with a calculation time divided by 4. Despite of the small error induce, it is then of interest to reduce the reflection order for calculations.

# APPROXIMATION OF WIND SPEED NEAR BARRIERS

## Introduction

Sound speed profile above real traffic noise configuration is usually varying due to topography and instabilities. However, most of reference models use a range independent sound speed profile. We study here the effect of this assumption. Calculations are achieved in inhomogeneous atmosphere using ATMOS [4] [5]. Wind speed evolution is computed with FLUENT, a flow numerical code.

## Configuration and results

We use an initial logarithmic sound speed profile:

$$c(z) = c_0 + v(z) \tag{1}$$

where $c_0$ is the reference sound speed and $v(z)$ the horizontal wind speed component given by:

$$v(z) = b \ln\left(1 + \frac{z}{z_0}\right) \tag{2}$$

with $b$ the refraction parameter and $z_0$ the rugosity length. Calculations are performed for a wind of 6 m.s$^{-1}$ 10 m high. Road traffic configuration and FLUENT results are presented Figure 6. Excess attenuation for range independent and evolutive wind speed profile is given Figure 7.

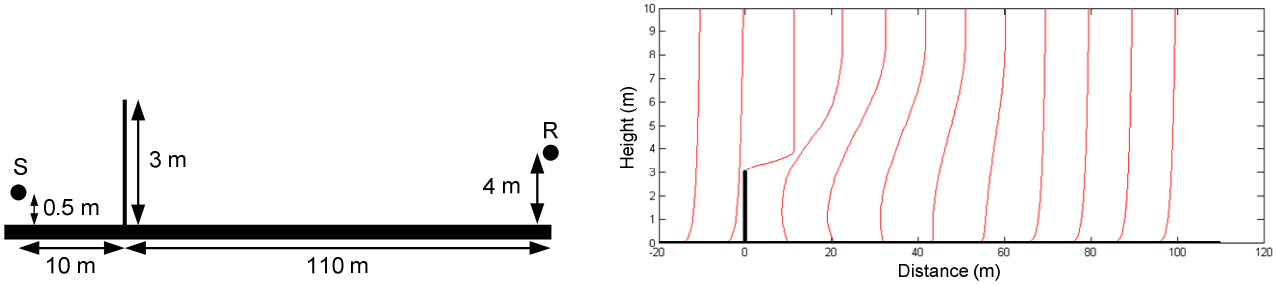


*Figure 6: Geometry of the road traffic configuration (left) and evolution of the sound speed profile computed with FLUENT*

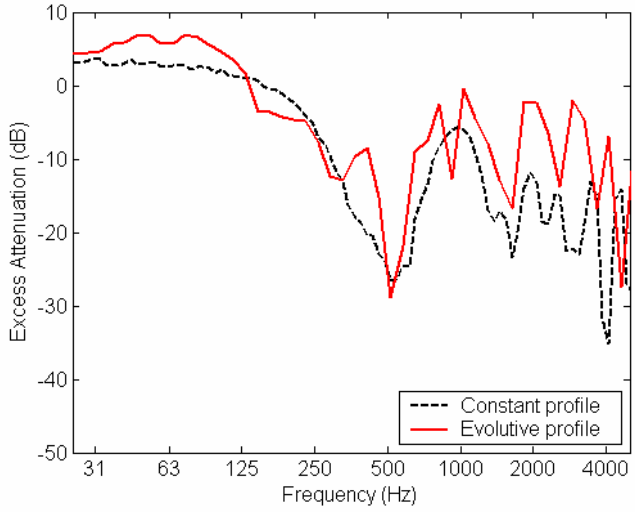


*Figure 7: Excess attenuation as a function of frequency for range independent and evolutive wind speed profiles*

### Discussion and conclusion

The main barrier effect on the wind is to accelerate this one above the barrier (Venturi effect) and to create a depression behind the obstacle (Figure 6). Those deviations generate high sound speed gradients which increase the acoustic level (Figure 7). Thus, the global excess attenuation for a normalized road traffic emission spectrum [3] is about **3 dB(A)** lower for the range independent than for the evolutive sound speed profile. The induced error is then significant so that it is important to take wind speed profile evolution into account to evaluate barrier efficiency.

## TWO-DIMENSIONAL APPROXIMATION FOR OBLIQUE PROPAGATION OVER A BARRIER IN PRESENCE OF A RAILWAY CARRIAGE SECTION.

### Introduction

We study here the common assumption which consists in achieving a series of 2D calculations instead of real 3D configuration. Some complete models exist but their running time is often important. It is then of interest to use 2D models to reduce calculation time. Calculations are achieved in a homogeneous atmosphere using MICADO [1]. MICADO can also perform calculations using a 2D½ BEM approach based on Duhamel's works [6] where the geometry remains infinite along one dimension with the possibility of including point or infinite incoherent line sources.

### Configuration and results

The aim is to predict sound propagation for a typical geometry with a noise barrier to focus on body-barrier effect in 2D compared to 3D. The configuration is described in Figure 8. The source representative of the wheel-rail contact is located at 0.1 m above the ballast. The receiver is placed 20 m from the barrier and 2 m high above the ground. Barrier, ballast and train are assumed to be acoustically rigid to simplify 3D calculation.

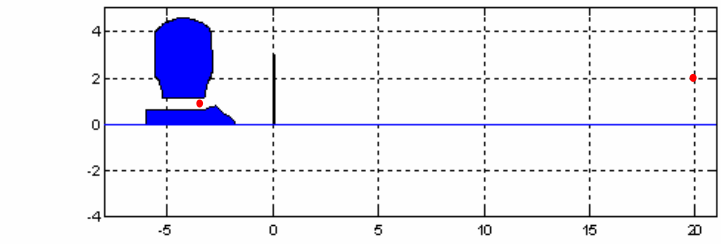


*Figure 8: Geometry of the configuration. S(-3.5,0.85) and R(20.0,2.2).*

The two-dimensional approximation for oblique propagation over a barrier is illustrated in Figure 9. The approximation corresponds to a rotation over the barrier such that it becomes normal to the propagation path.

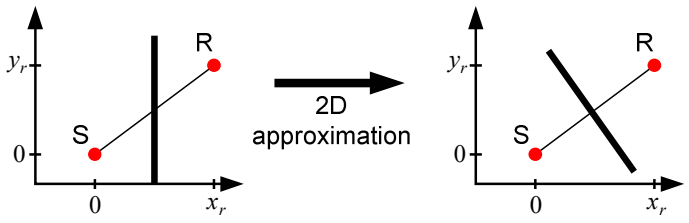


*Figure 9: Illustration of a two-dimensional approximation for oblique propagation over a barrier. The two figures are top views.*

Calculations are performed for $\arctan(y_r/x_r)$ of 0° and 45°. For an angle of 0°, the same configuration is used in 2D and in 2D½. Results are presented Figure 10. For an angle of 45°, the distance employed for the configuration used for 2D calculations has to be modified (Figure 11). Results are presented Figure 12.

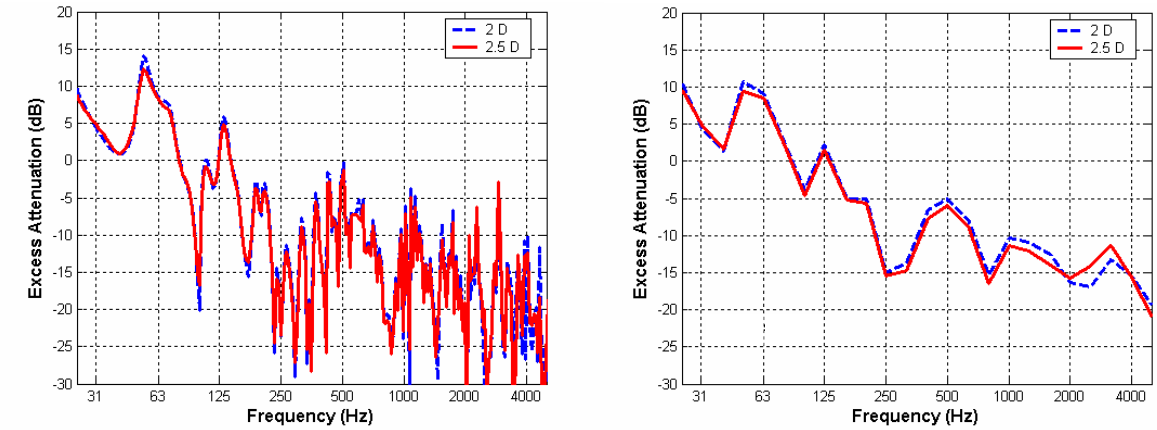


*Figure 10: Excess attenuation versus frequency for 2D and 2D½ BEM calculations for 0°. Results in narrow bands (left) and third octave band (right)*

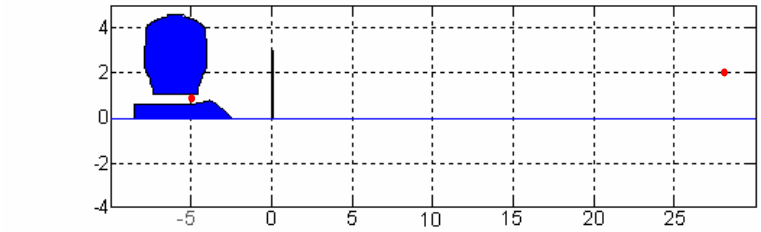

*Figure 11: Geometry of the configuration for an angle of 45°. S(-4.95,0.85) and R(28.14,2.0).*

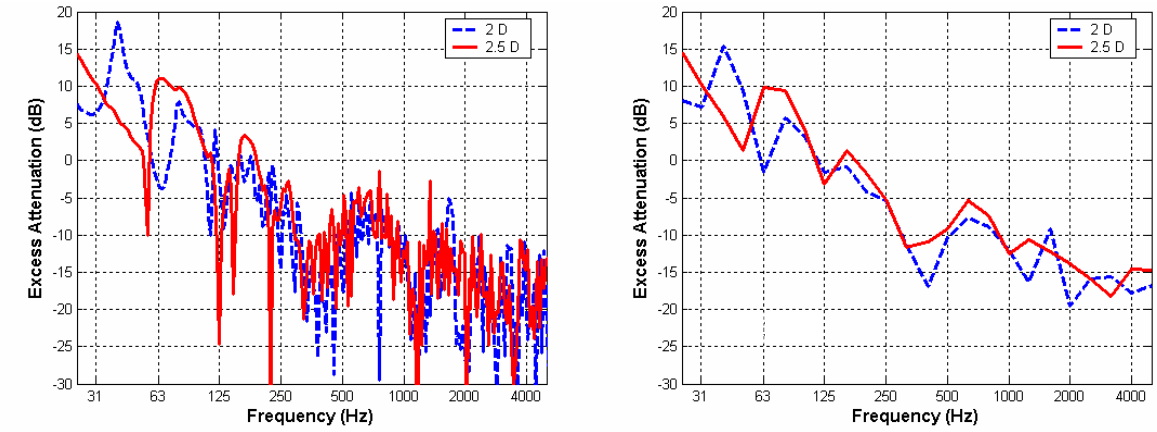


*Figure 12: Excess attenuation versus frequency for 2D and 2D½ BEM calculations for 45°. Results in narrow bands (left) and third octave bands (right)*

## Discussion and conclusion

The agreement between 2D and 2D½ results is very good in the case of a propagation perpendicular to the railway tracks direction. For the emission spectrum of a TGV rolling at 250 km/h, the 2D½ result is **0.4 dB(A)** lower than 2D result. It is poorer in the case of a 45° propagation; however the global shape of the 2D½ excess attenuation spectrum is quite well predicted by the 2D approximation, especially in the frequency range 500-4000 Hz where the railway noise is dominant. For the emission spectrum of a TGV rolling at 250 km/h, the 2D½ result is **0.9 dB(A)** higher than 2D result. The discrepancy between exact 2D½ and approximated 2D results is less than **1 dB(A)** in

terms of global attenuation. Thus the approximation of 3D propagation planes by 2D equivalent ones should be used with confidence in the reference model with a small error induced.

## LINEARIZATION OF SOUND SPEED PROFILES

### Introduction

Sound speed profile $c$ above real road traffic noise configuration may usually approximate by a logarithmic function:

$$c(z) = c_0 + b\ln\left(1+\frac{z}{z_0}\right) \tag{1}$$

where $c_0$ is the reference sound speed, $b$ is the refraction parameter, $z_0$ the rugosity length and $z$ the height. However a linear sound speed profile is used in many reference models:

$$c(z) = c_0(1+az) \tag{2}$$

where $a$ is refraction index. The aim of this part is to quantify the error due to this linear approach. Calculations are achieved in inhomogeneous atmosphere using ATMOS [4].

### Basis of the linearization of sound speed profiles

The linear profile is evaluate as an average sound speed profile using a Fresnel volume approach[7]. The sound speed profile can be estimated as a function of the average propagation height $h_m$ and the maximum width of the Fresnel ellipse $h_f$ (Figure 13):

$$h_m = \frac{{z_s}^2 + {z_r}^2}{2(z_s + z_r)} \tag{3}$$

$$h_f = \sqrt{\frac{\lambda}{4}\left(r+\frac{\lambda}{4}\right)} \tag{4}$$

where $\lambda$ is the wave length, $r$ the distance between source and receiver, $z_s$ the source height and $z_r$ the receiver height.

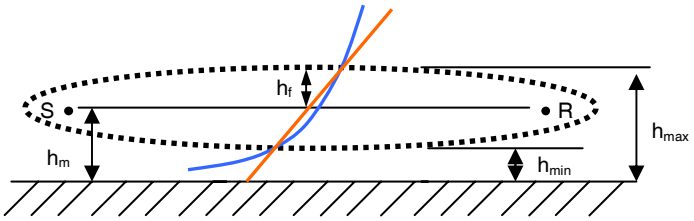


*Figure 13: Principle of the equivalent sound speed profile with the Fresnel volume approach*

Thus the average sound speed profile is determined between the heights $h_{\min}$ and $h_{\max}$ of the ellipse:

$$a = \frac{c(h_{\max}) - c(h_{\min})}{c_0 \cdot (h_{\max} - h_{\min})} \tag{5}$$

with $h_{\max} = h_m + h_f$, $h_{\min} = h_m - h_f$, $c_0$ the reference sound speed. $c(h_{\min})$ and $c(h_{\max})$ are two effective sound speeds at heights $h_{\min}$ and $h_{\max}$ :

$$c(h_{\min}) = c_0 + b \cdot \ln\left(1 + \frac{h_{\min}}{z_0}\right) \quad (6)$$

$$c(h_{\max}) = c_0 + b \cdot \ln\left(1 + \frac{h_{\max}}{z_0}\right) \quad (7)$$

When the source and/or the receiver are close to the ground, $h_{\min}$ becomes negative ($h_m < h_f$). For such cases $h_m$ keeps a minimal positive value $h_m = 2 \cdot h_0$ where $h_0$ is the average length of rugosity of elements ($h_0 = z_0 / 0.15$). Sound speed profiles depend of wind. Wind is fluctuating and irregular phenomenon so that realistic configurations need to be statistically studied:

$$u(t) = \overline{u} + u'(t) \quad (8)$$

where $t$ represents the time, $u(t)$ the instantaneous wind speed, $\overline{u}$ the average wind speed and $u'$ the fluctuating part of the wind speed. Principle of the method is to compute excess attenuations $EA_i$ for several wind speed associated with their apparition probability $p_i$. An average excess attenuation $EA_{av}$ is then easily got by:

$$EA_{av}(f) = \frac{\sum_i EA_i(f) p_i}{\sum_i p_i} \quad (7)$$

For long-term studies the Weibull law [8] is used to define the wind spread. The law for a wind speed of $2 m.s^{-1}$ 10 m high is presented Figure 14.

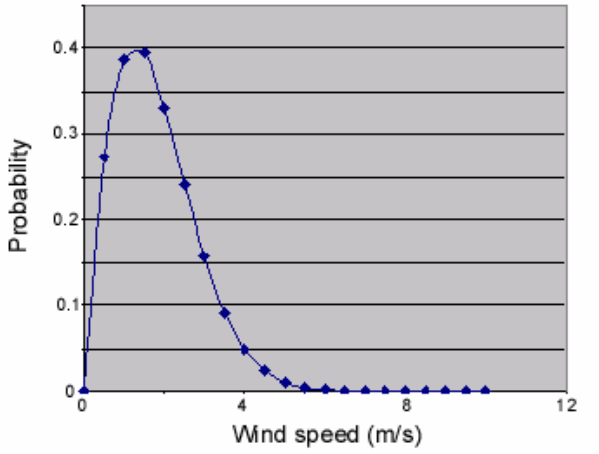


*Figure 14: Wind speed repartition with the Weibull law*

**Results**

The source is located at 0.5 m up to the ground. A 2 m high receiver is placed 250 m from the source. Excess attenuation computed with a logarithmic sound speed profile is compared with a variable linear sound speed profile and excess attenuation computed with long term logarithmic sound speed profile is compared with a variable linear sound speed profile averaged on the same period ( Figure 15).

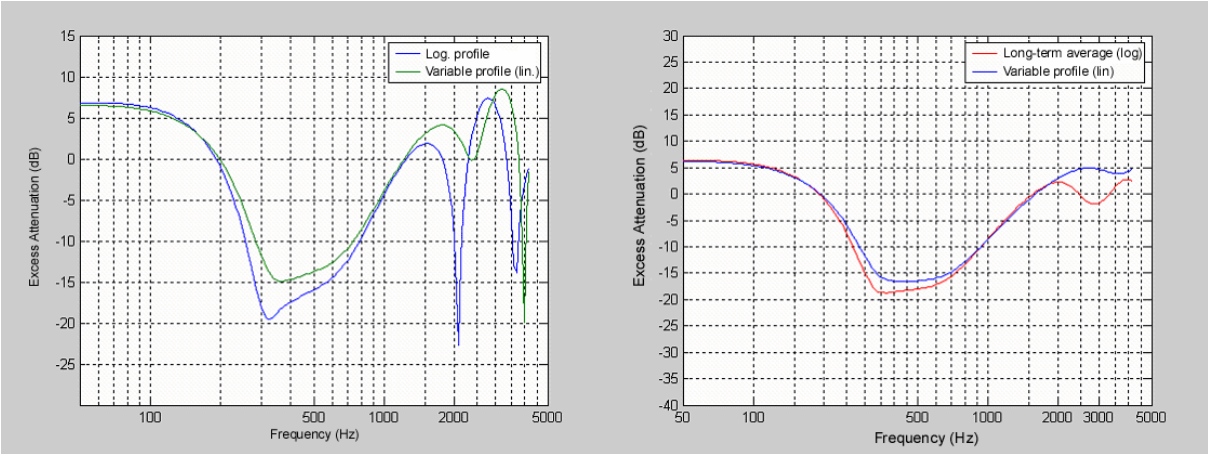


*Figure 15: Excess Attenuation for a logarithmic sound speed profile (left) and for an average long-term logarithmic sound speed profile (right) with a variable linear sound speed profile*

**Discussion and conclusion**

Comparison between excess attenuation computed with a logarithmic sound speed profile and with a variable linear sound speed profile points out an important deviation, especially at interferences location. However, the long-term logarithmic sound speed profile can be correctly approximated with a variable linear sound speed profile. The discrepancy between logarithmic and linear calculation is about **0.1 dB(A)** in terms of global attenuation for a long-term calculation for normalized traffic noise spectrum [3]. Since the agreement is good, this principle is an effective method to introduce average long-term logarithmic profile in the reference model. Using the analogy between sound propagation above a flat surface along curved ray paths and sound propagation above a curved surface along straight ray paths which allows to deal with linear profile [9], this approach is an alternative to take logarithmic sound speed profile in BEM calculations into account.

## BIBLIOGRAPHY

[1] P. JEAN - *A variational approach for the study of outdoor sound propagation and application to railway noise.* Journal of Sound and Vibration, 212(2), p. 275-294, **1998**

[2] M.E. DELANY, E.N. BAZLEY - *Acoustical properties of fibrous absorbent materials.* Applied acoustics, 3, p. 105-116, **1970**

[3] European Standard - *EN 1793-3, Road traffic noise reducing devices - Test method for determining the acoustic performance - Part 3: Normalized traffic noise spectrum.* **1997**

[4] F. ABALLEA, J. DEFRANCE - *Simple and multi-reflections using the PE method with a complementary Kirchhoff approximation*. Proceedings of 7ème Congrès Français d'Acoustique. Strasbourg, France, **2004.**

[5] F. ABALLEA, J. DEFRANCE - *Sound propagation over irregular terrain with complex meteorological effects using the parabolic equation model*. Proceedings of Inter-noise. Prague, Czech Republic, **2004.**

[6] D. DUHAMEL - *Efficient calculation of the three-dimensional sound pressure field around a noise barrier.* Journal of Sound and Vibration, 197, p. 547-571, **1996**

[7] A. L'ESPERANCE - *Modeling sound wave propagation in a natural complex environment (in French),* Thesis, Sherbrooke University, **1992**

[8] C. SACRE - *Physic of buildings handbook* (in French) Vol. 1. Paris: CSTB, **1995**.

[9] E. PREMAT, J. DEFRANCE - *Theoretical and experimental study of sound propagation for traffic noise*. Proceedings of 9th ICSV. Orlando, **2002.**